PHYSICAL REVIEW A VOLUME 26, NUMBER 4 OCTOBER 1982

Ionization of helium by fast, multiply charged ions. Deviations from a q^2 scaling

H. K. Haugen, L. H. Andersen, P. Hvelplund, and H. Knudsen
Institute of Physics, University of Aarhus, DK-8000 Aarhus C, Denmark
(Received 9 October 1981)

Experimental studies of the ionization of helium by fast, light ions have been carried out to investigate deviations from a q^2 scaling of the ionization cross section by ions of charge q. Systematic studies were performed for equivelocity H, He, Li, B, C, and O ions, carrying up to a maximum of three to four electrons, at reduced energies of 0.64, 1.44, and 2.31 MeV/amu. For ions of low charge, the results show good agreement with the theoretical work of Gillespie and Inokuti, who treat the deviations arising from ionic structure within the framework of the Bethe theory. In contrast, fully stripped ions of sufficiently high nuclear charge show deviations from a q^2 scaling, due to the failure of the first Born approximation. Such deviations from the first-order perturbative results were found to be well described by the qualitative approach of Bohr as well as by the three-state, close-coupling approach of Janev and Presnyakov.

I. INTRODUCTION

Inelastic atomic collisions at high velocities have long been described within the framework of the Bethe theory, based on the first Born approximation and on a sharp distinction of the projectile from the target. The theory, first put forth by Bethe[1] in 1930 and more recently reviewed by Inokuti[2] was for a long time restricted to the impact of structureless, charged particles on atoms and molecules. Recently, generalizations that incorporate high-velocity impact of atomic particles with electronic structure have been presented by Inokuti,[3] Nikolaev *et al.*,[4] and Gillespie.[5] They represent a natural extension of the Bethe theory and intrinsically include deviations from a q^2 scaling of the ionization cross section by ions of charge q due to their electronic structure.

However, deviations from a q^2 scaling may, in addition, arise due to the failure of the Born approximation. This is definitively demonstrated by the impact of bare nuclei at velocities insufficient to ensure an asymptotic interaction regime. A general theoretical treatment of such collisions is offered by the three-state close-coupling approach of Janev and Presnyakov,[6] who are able to treat the transition from the Bethe perturbative regime to the nonperturbative, strong-interaction regime. Collision phenomena, which fall outside the scope of the simple picture offered by the first Born approximation, are furthermore, familiar from the stopping power of fast ions in matter,[7] where the deviations have been given a qualitative physical interpretation.

The present work focuses on both of the above deviations from a q^2 scaling through an experimental study of collisions of light ions of H, He, Li, B, C, and O on a static helium target. The projectiles range from bare nuclei to ions carrying three or four electrons. To facilitate comparisons with theory, measurements were performed for equivelocity projectiles at reduced energies of 0.64, 1.44, and 2.31 MeV/amu, the highest energy representing a projectile velocity ~ 7 times a typical velocity of the target electron in the ground state. Experimental measurements determined the absolute sum of partial-ionization cross sections by the condenser-plate method and the relative contribution of singly and doubly charged ions by time-of-flight spectrometry.

II. EXPERIMENTAL TECHNIQUE

A rough schematic of the experimental setup is shown in Fig. 1 and has been described in some detail in a previous publication on ionization of helium by highly charged ions.[8] The new features include an improved gas cell with movable entrance and exit apertures and secondary-electron suppression by a grid of high transmissivity in the collection of the slow-ion current.

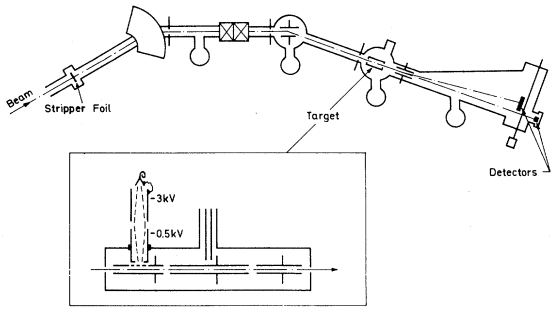

FIG. 1. Schematic diagram of experiment together with inset showing the target-gas cell.

The Aarhus EN tandem accelerator provided monoenergetic ion beams, which were charge-state analyzed by a 90° magnet and then passed on to the post-stripper region (Fig. 1), where the ions could be transmitted through carbon foils (5 $\mu g/cm^2$) to obtain equilibrium charge-state distributions. Subsequent magnetic analysis allows selection of the desired charge state, which is cleaned by electrostatic analysis before passing on to a gas cell for interaction with a static target gas. Analysis of the fast-ion beam components emerging from the gas cell includes electrostatic analysis together with detection by a position-sensitive solid-state detector, or measurements of the total current in a Faraday cup supplied with 200-V electron suppression.

The gas cell is indicated schematically in the inset of Fig. 1, while a photograph of the improved version used in the present studies is shown in Fig. 2. The gas cell is equipped with movable entrance and exit apertures (1 and 3 mm diameter, respectively), externally controlled by means of screw adjustments for horizontal and vertical motion. Ion

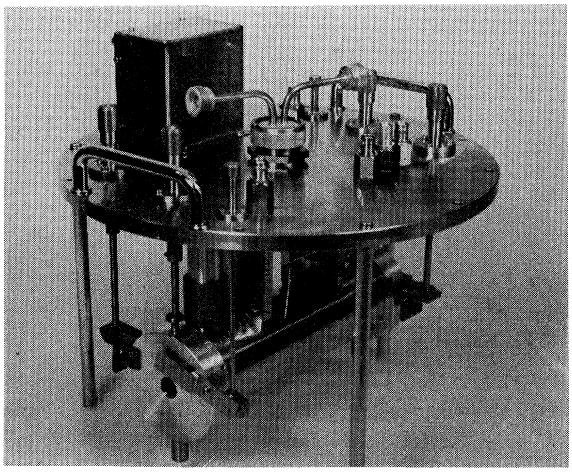

FIG. 2. Photograph of gas cell.

currents (unsuppressed) may also be measured immediately before and after the gas cell, the combined current measurements, and movable aperture system providing means to ensure full transmission of the fast ions. Experimental measurements were performed using condenser plates and a time-of-flight spectrometer. The latter uses single-particle detection by a channel-electron multiplier, which allows separation of the various charge states of the slow-reaction components. The total slow-ion-production cross section was determined by means of the condenser-plate method shown schematically in Fig. 3. The partial-ionization cross sections, with the charge-state integrity of the projectile maintained, dominate in the slow-ion production. In regard to comparison with theory, however, possible excitation of the projectile as well as stripping, are adequately incorporated into the theoretical calculations of Gillespie.[5] Capture, which is not included in this theory, may be assumed to play a negligible role.

In our earlier work,[8] a magnetic field was applied to the target region to suppress secondary electrons; in the present case, a wire grid of high transmissivity placed between the collision region and the collection plate (the top in Fig. 3) was held at a sufficient negative potential with respect to the latter to ensure an asymptotic behavior of the measured current. The plate configuration ensures a highly uniform field in the collision region so that the collection length is well defined. The grid shown in the figure is a mesh of 88% optical transmissivity placed on a rectangular support with a 5-mm border. The proper collection area of the top plate is therefore reduced by both the metal border and the mesh of the grid. To ensure that ions passing the 2-mm space between the guard plates and the grid did not contribute to the measured ion current, self-supporting copper foils attached to the guard plates were placed to block the slow ions entering the gap region. Currents were measured using Keithley 602 Solid-State Electrom-

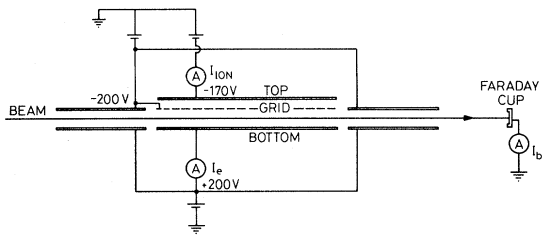

FIG. 3. Schematic of the condenser-plate method with the biasing potentials used in this study.

eters with doubly shielded BNC cables.

Although many of the aspects of the condenser-plate method have been discussed in the book of Massey and Gilbody[9] and references therein, investigations of experimental characteristics in the present work are presented here in some detail since they are complementary to those described in Ref. 9. Figure 4 shows the behavior of the collected ion current as a function of the applied field. (The plate potential should be multiplied by a factor of 2 to obtain the field strength.) In Fig. 4(a), no suppression field is applied between the grid and the collection plate, and a saturation is initially obtained at low collection field, in good agreement with the results of Gilbody and Hasted,[10] while at fields $\gtrsim 200$ V/cm, a gradual linear increase was observed. In Fig. 4(b), the collection plate was held 20 V positive with respect to the grid, and saturation is obtained at fields $\gtrsim 200$ V/cm whereafter a very small positive slope is obtained. In the interpretation of the observed characteristics, two important factors must be taken into account: The surface condition of significance in the ion-solid interaction is not well determined and cannot be directly compared with research on clean metal surfaces; the interaction of the slow ions in their rest gas represents (for most ions produced by fast light projectiles) a resonant interaction, He^+ in He, and is of nonnegligible magnitude even at pressures of a few mTorr. Kaminsky[11] reports on the role of surface contamination both on the magnitude and energy spectrum of secondary-electron emission by slow-ion impact on metal surfaces. In the present case, where the collection plate was Ni-coated brass, the explanation of the linear rise for the zero-suppression case depends on the influence of surface coverage on the potential and kinetic emission of secondary electrons. The small residual positive slope obtained even when 20-V suppression is applied can be attributed to charge-exchange phenomena of slow He^+ in the target gas prior to reaching the grid, since the fraction of charge-changing events not contributing to the current collected by the upper plate, is dependent on the collection field. This can be seen by taking for simplicity the case of single collisions in the collection process, where a charge-changing event taking place at the equipotential surface V_{top} below the grid will not be collected by the top plate after passing through the grid.

Figure 5 illustrates the characteristics of the suppression in two extreme cases, corresponding to collection fields of 80 and 400 V/cm. The arrows indicate where the potentials of the grid, top, and bottom plates are equal, and decreasing V_{top} corresponds to increasingly effective secondary-electron suppression. Figure 5(b) with $|V_{top}| = 170$ V was chosen in the present measurements since a well-defined saturation behavior was not found for substantially lower collection fields. The drop is very rapid, essentially becoming complete for suppressing potentials $\sim 5V$. This is in good qualitative

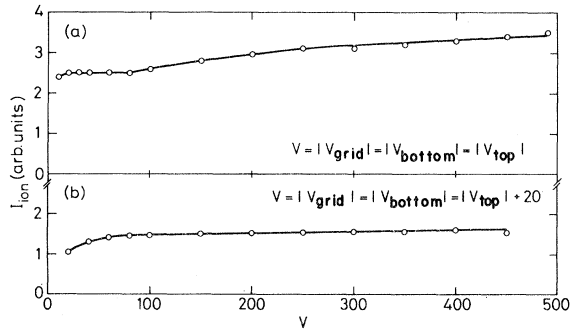

FIG. 4. Collection current to the TOP as a function of the applied potentials with (a) no suppressing voltage between the GRID and TOP, and (b) with 20-V suppression. Data obtained for 4-MeV $He^{2+} \rightarrow He$ with $p \sim 5 \times 10^{-3}$ Torr, but conditions for (a) and (b) are not exactly identical.

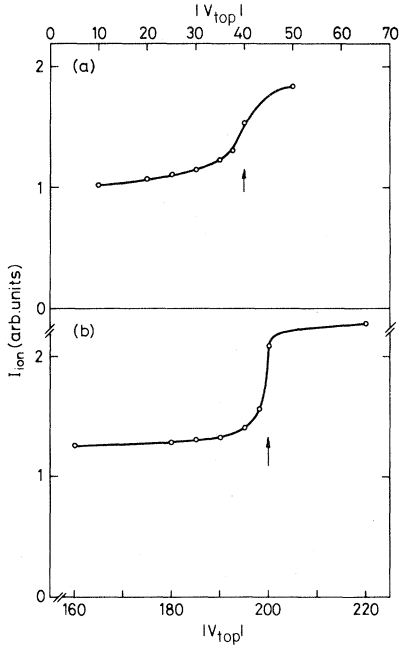

FIG. 5. Characteristics of the suppression at constant collecting field for same reaction as Fig. 4. The arrows indicate where the potential on the TOP is identical to that on the GRID. Lower $|V_{top}|$ thus indicates increasingly effective secondary-electron suppression.

agreement with Kaminsky, who indicated a degradation of the secondary-electron energy spectrum as a result of surface coverage, as well as with the experiment of Gilbody and Hasted,[10] although in their case, impact of Ar^+ on gold could be expected to lead to secondary electrons of lower energy. The weak dependence on suppression potential for $|V_{top}| \lesssim 190$ V is due to the secondary-collision processes taking place below the grid. It should also be noted that the total initial drop upon application of a suppressing potential is not solely attributable to the secondary-electron emission but also to the secondary collisions taking place between the grid and the top plate, where a very small positive potential of the latter with respect to the grid can be expected to lead to collection by the grid. This is clearly illustrated in Fig. 6, where extrapolations of the normalized current (divided by pressure) are shown as a function of the target thickness for suppressing potentials between the grid and top plate of 30 and 100 V. The opposite slopes of the grid and plate current indicate the preferential collection of secondary slow ions by the grid. Dependence on the potential difference is also seen, but the same cross section is obtained in the limit of zero pressure. This clearly emphasizes the inherent dangers of investigation without pressure extrapolation, since although projectile related cross sections are negligible in most cases at these high velocities, resonant capture by the slow ions requires extremely low-target thicknesses or, alternatively, independent investigation of the pressure behavior. The latter has been well accounted for by taking the magnitude of the cross sections for resonant He^+-He charge exchange into account.[12]

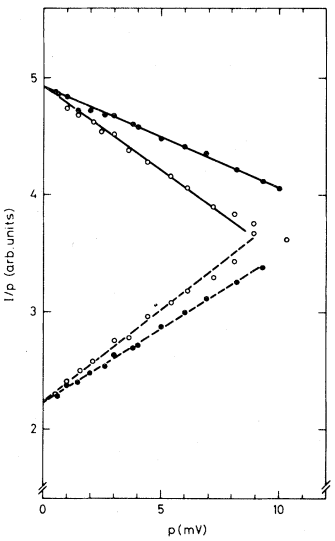

FIG. 6. Pressure dependence of the current to the the TOP (solid) and the GRID (dashed) as a function of target pressure. It is seen that two different suppressing potentials of 30 V (●) and 100 V (○) yield the same cross section.

Since the present investigations attempt to cover in a systematic way the ionization of helium by a number of isoelectronic projectile species, a great demand is placed on the technology of ion production. Since the present system cannnot produce all the desired ions over the energy regime of interest at sufficient intensity to allow use of the condenser-plate method, such measurements were performed for each species, where large currents could be obtained coupled with time-of-flight spectrometry, using a considerably defocused primary beam. This served to calibrate the efficiency of the spectrometer system, which then was used for ion beams of low intensity. The spectrometer samples a ~ 5 mm length of the interaction region, from where the slow ions produced are focused into the channeltron held at -3 kV. The characteristics of the spectrometer system are discussed in considerable detail in part II of this study,[13] where the relative efficiency of the system for ions of noble gases of varying charge states was considered. In the present case, the situation is far less critical in that nearly all ionizing events lead to single ionization, and any errors would be expected to be the same for all ions in so much as the fast beam and spectrometer are uncoupled (that is, the recoil distribution is not of experimental significance). That the average efficiency of the system is $\sim 97\%$ (taking into account the sampling length and target density) indicates that collection and detection of the slow ions are optimum.

Finally, some comments regarding the relative magnitude of the number of singly and doubly charged recoils are in order. With reference to part II,[13] it will be seen that for ions of low-charge multiplicity, double ionization of helium in the energy regime of interest is $\lesssim 1\%$. This may clearly be neglected in our comparisons with the Bethe theory. While the double-ionization fraction increases strongly with q, the theoretical treatments of ionization by multiply charged ions are sufficiently qualitative to again render this contribution irrelevant.

We conclude this section with a summary of uncertainties in our measurements. The condenser measurements had contributions from the follow-

ing sources: the effective collection length of 7.02 ± 0.25 cm, the pressure calibration for helium gas of 0.88 ± 0.02 mTorr/mV, and $\sim 2\%$ indeterminacy on the required intercept of the pressure extrapolation (see Ref. 8), leading to an overall uncertainty of $\sim 5\%$. The time-of-flight measurements were used to determine the ratio of double-to-single ionization, as well as abolute cross sections for weak primary beams (hence precluding the condenser technique) after the calibration of the spectrometer efficiency. While the above comment on efficiency referred to a design collection length, it must be taken into account that for various ion beams, this spectrometer constant is uncertain by $\sim 4\%$. Taking into account the indeterminacy on the time-of-flight extrapolations, which were typically $\sim 8\%$, the total for these latter measurements is $\sim 9\%$. Thus, the results to be presented later have associated uncertainties within a range $\sim 5-10\%$.

III. THEORETICAL BACKGROUND

A. Bethe theory and immediate extension

Since the Bethe theory has been familiar to the literature of atomic collisions since 1930 and has been reviewed both in its general features and in connection with experiment by Inokuti,[2] the following will represent solely a short overview of the most important aspects and a brief discussion of the extension to structured projectile ions. The description of "fast" collisions, where the distinction between fast and slow rests on a comparison of the relative magnitudes of the projectile- and target-electron velocities, is treated within the first Born approximation by the Bethe theory. The elegance of the approach lies in its relative simplicity and conceptual clarity, the import of the formalism lying in the preservation of the distinct individuality of the projectile and target system. In the first Born approximation, the differential cross section for inelastic scattering of a particle of velocity v, mass M_1, and charge qe with a stationary atom of mass M_2 may be expressed

$$d\sigma_n = 2\pi q^2 e^4 (mv^2)^{-1} Q^{-1} \mid \epsilon_n(K) \mid^2 d(\ln Q) , \tag{1}$$

where

$$Q = (\hbar K)^2/2m ,$$

$\hbar\vec{K} = \hbar(\vec{k} - \vec{k}')$ being the momentum transfer and

$$\epsilon_n(\vec{K}) = \left\langle n \left| \sum_{j=1}^{Z} \exp(i\vec{K}\cdot\vec{r}_j) \right| 0 \right\rangle = \int u_n^* \sum_{j=1}^{Z} \exp(i\vec{K}\cdot\vec{r}_j) u_0 \, d\vec{r}_1 \cdots d\vec{r}_Z$$

is an atomic matrix element. The cross section is thereby represented as a product of the Rutherford-scattering probability and the conditional probability of a given transition upon receiving momtentum $\hbar K$. The matrix element $\epsilon_n(\vec{K})$ is termed the form factor and is well known in many areas of physics, where the structure of the object is to be described. In atomic physics we generally deal with the oscillator strength as introduced by Bethe

$$f_n(K) = \left[\frac{E_n}{R} \right] (Ka_0)^{-2} \mid \epsilon_n(K) \mid^2 , \tag{2}$$

where R is the Rydberg energy and

$$a_0 = \frac{\hbar^2}{me^2} .$$

The oscillator strength provides the connection between fast collisions and photoabsorption, that is, the limit of the oscillator strength as $K \rightarrow 0$.

The integration of Eq. (1) over Q requires a consideration of the kinematics of the collision. For a structureless charged particle, the integrated cross section for ionization has the form

$$\sigma_i = \left[\frac{4\pi a_0^2 q^2}{T/R} M_i^2 \ln\left[\frac{4c_i T}{R} \right] + \frac{\gamma_i}{T/R} + O\left[\frac{R^2}{T^2} \right] \right] , \tag{3}$$

where

$$M_i^2 = \int_{I_1}^{\infty} \left[\frac{R}{E} \right] \left[\frac{df}{dE} \right] dE , \tag{4}$$

I_1 being the ionization potential. The factor M_i^2, termed the dipole matrix element squared for ionization, is determined by the density of the oscillator strength (df/dE) in the continuum. This is precisely an example of the connection with photoionization noted above and corresponds to the distant collisions (large impact parameter), where a Fourier analysis of the field would lead to an approximate physical description of the absorption of virtual field quanta (see, e.g., Ter-Mikaelian[14]). The factors c_i and γ_i result from the integration, the γ factor becoming important at lower velocities. The important features of the integrated cross sections are best shown in a diagram, commonly termed the Fano plot, where $(T/R)\sigma_i(4\pi a_0^2 q^2)^{-1}$ is

plotted versus $\ln(T/R)$. Asymptotically, the plot gives a straight line of slope M_i^2 and an intercept related to $M_i^2 \ln c_i$, thus revealing the important physics while eliminating the uninteresting scalings related to Rutherford scattering.

The extension of the theory to ions with ionic structure was initiated by Inokuti[3] and follows naturally from the preceding formalism. On this basis, Gillespie[5] has performed calculations for ionization of hydrogen and helium by fast light ions along the above lines, using an integrated cross section of the form

$$\sigma_i = 4\pi a_0^2 \frac{\alpha^2}{\beta^2}\left\{q^2 M_i^2\left[\ln\left[\frac{\beta^2}{1-\beta^2}\right]-\beta^2\right]+c_{\mathrm{el},i}+2I_{\mathrm{in},i}+(\gamma_{\mathrm{el},i}+2\gamma_{\mathrm{in},i})\alpha^2/\beta^2\right\}. \tag{5}$$

α is the fine-structure constant and $\beta = v/c$, q is the net ionic charge, and the use of β in Eq. (5) reflects simply the relativistic formulation as opposed to the nonrelativistic one presented earlier. The parameters $c_{\mathrm{el},i}$, $I_{\mathrm{in},i}$, $\gamma_{\mathrm{el},i}$, and $\gamma_{\mathrm{in},i}$ include properties of both colliding partners, the last two factors giving the deviation of a Fano plot from a straight line at lower velocities.

B. Bohr's qualitative treatment

Although the following treatment is not rigorous, it serves as a simple semiquantitative treatment of collisions, which in addition offers an immediate extension to treatment of high ion charges of interest in the present paper. Following Bohr,[15] the nature of the collision between the ion and a target electron is to a large extent determined by the value of the parameter $\kappa = 2qv_0/v$. If $\kappa > 1$, a classical orbital picture is valid, while if $\kappa < 1$, the wave description of the scattering applies. The very important point is that spatial coordinates do not enter the parameter κ so that the alternative descriptions are valid for all parts of the field or not at all, as long as the field is Coulombic. The above discussion thus concerns the pure Rutherford scattering of two charged particles. In atomic collisions, however, the binding forces play an important role, and an appropriate description of atomic collision phenomena must recognize that the phenomena are many body in nature. At a very early stage, Bohr[16] identified the essential parameters as those which connected with the dynamical, not the spatial, characteristics of the atomic system. Thus limitations on energy transfer arise when the collision time becomes comparable to the atomic period, such that larger impact parameters lead to adiabatic encounters.

The important feature of time variations was incorporated by Bohr through the parameter

$$\eta_s = \frac{2v}{u_s},$$

where u_s is the velocity of an active atomic electron of ionization potential I_s. The various regimes of classification thereby follow from consideration of the absolute magnitude of κ and the relative magnitude of κ and η. In general, the collisions are divided into two classes: free and resonant, corresponding, respectively, to close and distant collisions. The physical basis for this division is that, for close collisions, the binding can be expected to play a minor role, whereas the treatment of distant collisions rests on correspondence arguments—the sum of the strengths of the virtual atomic oscillators is equivalent to that of one free electron. The approach provides a simple and physically intuitive picture, which is quite accurate but not rigorous since the interaction is never strictly Coulombic.

Bohr proceeds by dividing the relevant average energy transfers obtained on a classical treatment by the ionization potential to determine the number of ionization events ω_I. He obtains

$$\omega_I = \frac{2\pi N \Delta R q^2 e^4}{mv^2} \times \sum_s \frac{1}{I_s}\left[\left[\frac{\kappa}{\eta_s}\right]^{-1} + 2\delta_s \ln(\eta_s[\kappa]^{-1})\right], \tag{6}$$

where $N\Delta R$ represents the target thickness and δ_s describes the distribution of the energy transfer over various kinds of inelastic transitions. The square brackets have the special significance that where the enclosed quantity is less than 1, the value of the bracket is replaced by unity.

The entirety of inelastic phenomena is not of direct interest in the present paper, and the reader is referred (for a discussion of very strong interactions) to Bohr, whose semiquantitative description was used by the present authors in analysis of ioni-

zation by highly charged ions.[8] For the present, the regimes of interest are represented by $\kappa < 1$, $\eta > 1$, and $\eta > \kappa > 1$. The first case corresponds to a strictly perturbative regime, where the square brackets of Eq. (6) are replaced by unity and the pure q^2 scaling of the Bethe theory is obtained. The second case is of greatest interest in the present work since it reflects on the transition from a perturbative to a classical regime. For the sake of concreteness, Eq. (6) is expressed for the ionization cross section of helium,

$$\sigma_i = 8\pi a_0^2 \left[\frac{v_0}{v}\right]^2 q^2 \left[\frac{I_H}{I_{He}}\right] \times \left\{1+0.9\ln\left[\left[\frac{v}{v_0}\right]^2 \frac{1}{q}\left[\frac{I_H}{I_{He}}\right]^{1/2}\right]\right\}, \tag{7}$$

where I_H and I_{He} are, respectively, ionization potentials of hydrogen and helium. The appearance of q^{-1} in the logarithmic term leads to a decrease in the cross section for large q relative to the Rutherford scaling. Qualitatively this relates to the decreasing role of resonance effects, which totally disappear when $\kappa = \eta$.

C. Janev's close-coupling treatment

The transition from the perturbative regime to a strong-interaction regime is effected by both increasing the ionic charge and decreasing the ion velocity as q and v are coupled in the quantity κ. This intermediate (strong-interaction) regime generally presents a complex problem since it becomes necessary to take into account several effects of comparable magnitude. As the interaction is strong, but at the same time $v \sim v_0$, neither of the two conceptual formulations, molecular orbital and first-order Born approximation, strictly applies in the intermediate region. In general, it is here that coupling to many intermediate states becomes significant, and simplification can only result from a choice of representation which takes into account the essential features of the coupling.

With respect to the entirety of collision phenomena, encounters with $v << v_0$ are dominated by charge exchange, while for $v >> v_0$, capture becomes a highly unlikely process, falling off in the asymptotic limit as $\sim v^{-12}$. In the intermediate region, excitation and ionization are comparable in magnitude to capture, while the dominance of the former attains rapidly in the transition from $v \sim v_0$ to $v > v_0$. Thus, in comparison with Gillespie's calculations at higher velocities, capture may be assumed by play a negligible role, while an adequate theoretical model for the intermediate regime must differentiate the contribution of direct ionization to the continuum and capture into bound states.

The approach of Janev[17] is based on the approximate solution of two- and three-state-coupled equations, where the ion-atom interaction is treated within a dipole approximation. The work is of interest in the present context in the description of collisions of multiply charged projectiles, where the interaction is sufficiently strong that the assumptions of the Bethe theory are not fulfilled. In these cases, a description of the interaction may be carried out in terms of multipole components since the main contribution to transition probabilities come from relatively large distances, greater than atomic dimensions. Denoting the vector describing the internuclear axis as $\vec{R}(t)$, and $\vec{r}$ as the position of the active electron, we may write the interaction as

$$V(\vec{r},\vec{R}) = -\frac{qe^2}{|\vec{R}(t)-\vec{r}|}, \tag{8}$$

the long-range part of which is the dipole potential

$$V(\vec{R},\vec{r}) \simeq -q\frac{\vec{d}\cdot\vec{R}}{R^3}e^2, \tag{9}$$

where $\vec{d}$ is the dipole moment.

The set of coupled equations obtained from Schrödinger's equation with the associated atomic basis expansion is of the form

$$i\hbar\frac{da_n}{dt} = \sum_{s\neq n} a_s V_{ns} e^{i\omega_{ns}t}, \tag{10}$$

where

$$\hbar\omega_{ns} = E_n - E_s$$

and V_{ns} are the matrix elements of the interaction

$$V_{ns} = \int \varphi_n^*(\vec{r}) V(\vec{R},\vec{r}) \varphi_s(\vec{r}) d^3\vec{r}. \tag{11}$$

In an earlier paper, Janev and Presnyakov[6] obtained the following form for an excitation cross section:

$$\sigma_{ex} = 2\pi \int_0^\infty \rho\, d\rho\, W(\rho,v,q\lambda,\omega) \tag{12a}$$

$$= 2\pi(q\lambda/\omega) D(\beta), \tag{12b}$$

where W is the transition probability, ρ the impact parameter, $\hbar\omega$ the energy difference of the per-

tinent states, and λ is related to the oscillator strength by

$$\lambda=\left[\frac{f_{01}}{2\omega}\right]^{1/2}, \tag{13}$$

f_{01} being the oscillator strength of the transition. The function $D(\beta)$ incorporates the associated integrals for the transition probabilities and is tabulated in Ref. 16. The extension from excitation to ionization follows from consideration of an effective continuum oscillator strength such that the continuum is thereby replaced by an effective energy level so that f_{01} in Eq. (13) is replaced by f_{eff}.

The total transition probability is the sum of direct contributions and transitions through the resonance level. Specifically

$$W_j=W_{0\to c}+\tfrac{1}{4}W_{0\to r}W_{r\to c}\ , \tag{14}$$

where r represents the intermediate level and c the continuum. Assuming that $W_{r\to c}\sim\frac{1}{2}$ for all significant impact parameters, the cross section on the basis of (12b) becomes

$$\sigma=2\pi q\xi\left[\frac{\lambda_c}{\omega_c}D(\beta_c)+\frac{1}{8}\frac{\lambda_r}{\omega_r}D(\beta_r)\right], \tag{15}$$

the two terms representing, respectively, the contribution of the direct transfer to the continuum and via the resonance level, and the factor ξ representing the number of active electrons in the atom. Specific values of the λ and ω parameters are given in Ref. 6, where it was determined that the second term represents a generally small contribution ($\lesssim 15\%$). On the basis of this simplified model, it is possible to represent the cross section in a universal way as a function of the reduced quantities $\tilde{\sigma}=\sigma/q$ and $\tilde{E}=E/q$, where E is measured in energy/amu.

IV. EXPERIMENTAL RESULTS AND DISCUSSION

A. Comparison with calculations of Gillespie

The results of Gillespie[5] for ionization of helium, using a direct extension of the Bethe theory, are shown in Fig. 7 together with experimental data obtained in this study. It can be seen that the agreement with theory is very good, and the experimental uncertainty, which is of order $5-10\%$, does not allow determination of deviations within this latitude. The work supplements, with a superior apparatus, the preliminary investigations of our earlier work[8] and extends the investigation to lithium, where the increase in cross section for Li^{2+} with respect to He^{2+} is in good agreement with the predictions of Gillespie. Cross sections for Li^{+} at the reduced energies of 0.64 and 1.44 MeV/amu were also determined, both yielding 6.41 units on the Fano plot of Fig. 1, but have not been included due to our serious doubts concerning the nature of the Li^{+} beam. In particular, it is suspected that the beam used contained a significant metastable component which, due to decreased screening, would lead to an enhancement of the ionization cross section.

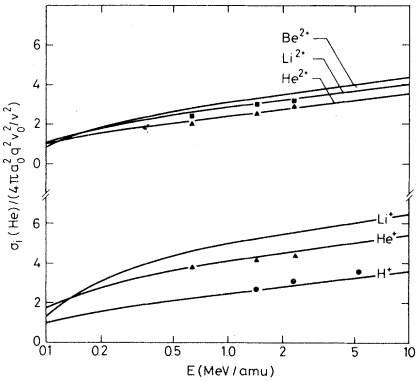

FIG. 7. Fano plot showing comparison of present experimental data for H (●), He (▲), and Li (■) ions with the calculations of Gillespie.

Hvelplund[18] has investigated capture and loss processes for ground-state and metastable Li^{+} in helium and argon targets in the energy range $40-90$ keV. In that regime, capture takes place largely to excited states, all of which rapidly ($\lesssim 50$ ns) decay with the exception of $1s2s\,{}^1S$ and $1s\widetilde{2s}\,{}^3S$. Although the velocity in the present case is considerably higher ($\sim 5-8v_0$), alternative means of production of Li^{+} either by post stripping or charge exchange could not guarantee a negligible contribution from metastables.

With respect to extensions of investigations of the Bethe theory for structured projectiles to include heavier isoelectronic ions, certain points should be recognized. First, as will be discussed in some detail below, projectiles of higher charge (here, $q>3$) rapidly break the conditions for a perturbative interaction since at constant v, the Coulomb scaling is q^2. Second, heavier ions carrying many electrons do not offer convenient possibilities for such investigations because matrix-element calculations are complicated and because

the unscreened interactions at small impact parameter give difficulties related to the first point above.

B. Deviations from a q^2 scaling for high-q projectiles

The results reported for H, He, and Li ions were found to be well supported theoretically and hence described by the first-order perturbation theory. The transition to high charge states inevitably leads to a breakdown in the predictions of the Bethe theory, notably deviations from the q^2 Coulomb scaling at constant velocity. This is illustrated in Fig. 8 for bare projectiles up to oxygen at the three reduced energies of this study. The experimental data are compared with the Bethe theory (Gillespie) as well as the qualitative treatment of Bohr and the close-coupling calculations of Janev.

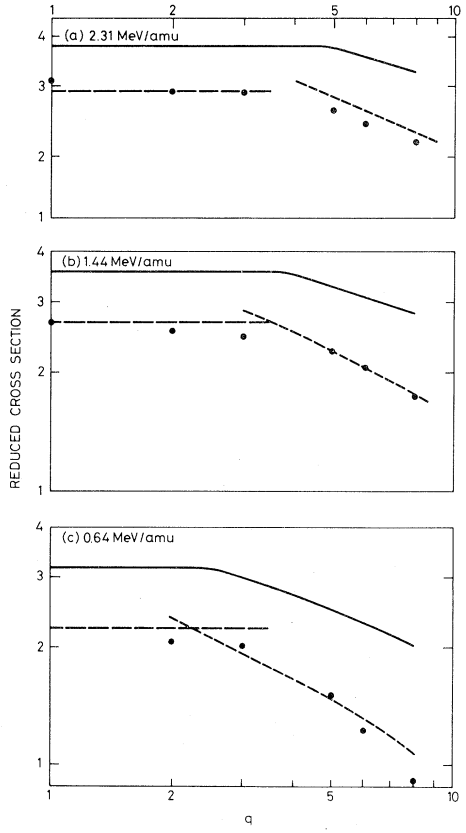

FIG. 8. $\sigma_i/(4\pi a_0^2 q^2 v_0^2/v^2)$ for incident bare projectiles at three reduced energies. Points represent experimental data, while the theoretical models of Bohr (solid), Janev (short dash), and Bethe (long dash) are indicated as continuous curves.

It can be seen that within the experimental uncertainty of 5—10%, the predictions of perturbation theory remain valid up to $q \sim 3$. Thereafter the cross section drops below that which would be predicted by the Bethe theory. Furthermore, the results for fully stripped ions of boron, carbon, and oxygen are seen to be well described by the close-coupling calculations of Janev. At the two highest velocities, the reduced proton cross section is higher than that obtained for He^{2+} and Li^{3+}, but the difference cannot be concluded to be significant on the basis of the present experiment.

In Fig. 8, the transition between the two regimes, $\kappa < 1$ and $\kappa > 1$, is illustrated by the deflection in the solid curve, which occurs at $\kappa = 1$, in excellent agreement with the experimental data. The decrease is attributable to the diminishing role of resonance effects, which is reflected in Eq. (7) by the inverse power of the ionic charge in the logarithm. For purposes of comparison, the more formal approach represented by the work of Janev will be discussed below, where the transition to the cross-section maximum and consideration of the role of capture is treated in some detail.

Figure 9 illustrates the results for the heavier ions which carry electrons. The interpretation is

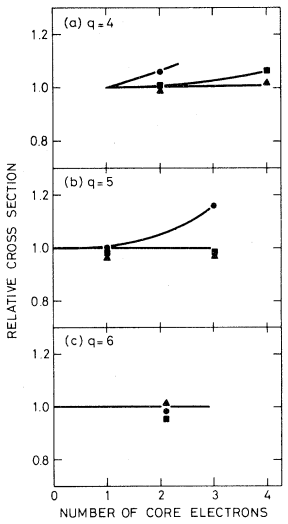

FIG. 9. Single-ionization cross sections for multiply charged ions with electronic structure. The results are normalized for $q=4$ to the B^{4+} data, whereas the $q=5$ and 6 results are normalized to the corresponding cross sections for bare nuclei. The results are shown for three reduced energies, 0.64 (▲), 1.44 (■), and 2.31 MeV/amu (●).

not totally straightforward in that the size of the effect shown here is small, while the collision regime can no longer be considered asymptotic. However, the structured heavier ions fit well into the close-coupling scaling, which treats the interactions in a simplified way. The import of Fig. 9 can thus be considered semiempirical in nature. Indicated trends, which are statistically significant, follow from simple physical arguments. Thus, the screening effects are of greatest significance for the lower charges and at higher velocities, where the ionic structure cannot be totally neglected. At $q=6$, however, no difference can be noted between C^{6+} and O^{6+} at any of the reduced energies.

C. Transition to the strong-interaction regime

The deviations from a q^2 scaling noted above reflect the transition to a strong-interaction regime (the so-called stopping-power maximum in penetration theory), indicating that the multitude of collision phenomena contributes strongly to the energy loss of the incident projectile. This is indicated in Bohr's formulation by the increase in κ with increasing charge state, qualitatively explaining the inapplicability of a perturbation treatment for the larger-q ions of this study. It need hardly be emphasized, however, that Bohr's criteria are only approximate and the boundaries of the various regimes ill defined. This is further qualified by the degree of precision required and, more importantly, by the nature of the questions asked. This point will become more clear in part II of this study, where high-velocity inelastic processes of a specific nature are discussed. For the present, it is attempted to take the deviations into account in a universal way and further extrapolate the work to lower velocities where capture plays a significant role.

Figure 10 shows the present experimental results for the various multiply charged ions ($q \gtrsim 3$) as a function of the reduced parameters suggested by Janev. Also shown are the predictions of Bohr[15] and Olson,[19] where, in contrast to those of Janev, the sum of capture and ionization is determined. The results of Olson stem from Monte Carlo classical-trajectory calculations, which give the well-known E^{-1} dependence at high energies. The agreement between the three-state close-coupling treatment of Janev (outlined in Sec. III C) and the experimental data for multiply charged ions is seen to be excellent, and the extensions to even lower reduced energies than those reported above show that the area of the maximum is well described. The latter region was investigated by coincidence measurements, in which the charge-state integrity of the ionizing projectile was ensured, for multiply charged B and C at 0.19 and 0.13 MeV/amu. For purposes of comparison, B^{5+} at 0.19 MeV/amu had a total single-ionization cross section of 7.4×10^{-16} cm^2, while that corresponding to B^{5+}, maintaining its original charge state during the collision, gave 6.3×10^{-16} cm^2; while for 0.13-MeV/amu C^{5+}, the same cross sections were 8.3×10^{-16} and 4.6×10^{-16} cm^2, respectively. Clearly, this difference between pure and total ionization rapidly diminishes with increasing velocity, which in a crude mechanistic picture of capture at high velocity is associated with the difficulty of transferring sufficient momentum to the electron in a spatial solid angle closely associated with the projectile. Thus the points above the maximum have a very minor contribution from capture into bound states, indicating that although the magnitudes obtained by Olson and Janev in the region $100-200$ (keV/amu)/q are essentially the same, the difference in scaling can be considered significant.

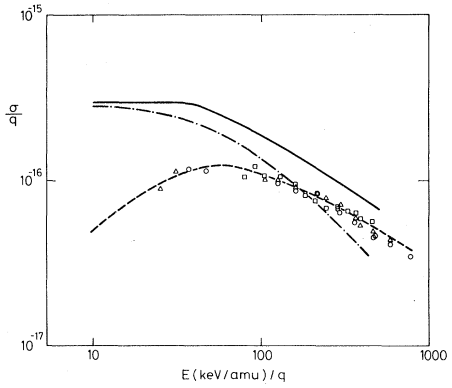

FIG. 10. Reduced cross section for ionization of helium. Bohr (solid line) and Olson (dot-dash) give total target electron loss. Janev (dash) gives solely the contribution from ionization to the continuum. Experimental points of the present study for C (△), B (○), and O (□) ions ranging in charge state from 3 to 8 exclude capture into bound states of the projectile.

Before concluding this section, some comments are in order concerning the validity and generality of the theoretical treament. Although Janev and Presnyakov[6] have shown their approach to give reasonably good agreement for proton-atomic-hydrogen collisions on the basis of the simplifying assumptions introduced via the dipole approxima-

tion, it would be expected that such a theoretical approach is better justified for the strong perturbing fields of the highly charged species. Such is indicated from this study, although recent work on collisions between fast, multiply charged ions and atomic hydrogen in the regime 12–195 keV/amu by Shah and Gilbody[20] indicates that for this target, the work of Janev and Presnyakov significantly underestimates the cross section at 145 keV/amu, while the classical-trajectory calculations of Olson and Salop[21] are in good agreement.

What is determined in a measurement of ionization with projectile-charge integrity maintained is the sum of all contributions with the exception of capture into bound states. In a way which is necessarily rather arbitrary, theory divides ionization into direct and "capture-to-the-continuum" components, where in the latter case, the ionized electron is closely associated with the projectile. Capture to the continuum can be expected to give a significant contribution to the ionization cross section over a restricted energy range. For proton impact on atomic hydrogen, Shakeshaft[22] has performed coupled-state calculations using 35 functions centered on each proton and obtained the separate contributions for direct ionization and charge transfer to the continuum. Thus, Shakeshaft takes the entirety of transfer channels into account in an approximate but *explicit* way, whereas the three-state close-coupling theory of Janev associates ionization solely with discrete and continuum oscillator strengths. On the other hand, classical-trajectory calculations allow determination of all contributions within the limits of the classical formulation but fail at high energies for reasons that become obvious on the basis of the correspondence arguments of Sec. III B. In conclusion, although it is expected that much of the essential physics of the transition to the stopping-power maximum is illustrated by the simple close-coupling treatment of Janev, the simplifying assumptions and latitude in the choice of the intrinsic parameters should be kept in mind in comparison with more rigorous calculations, or where processes of a specific nature are of interest.

V. CONCLUDING REMARKS

A systematic study of ionization of helium by fast, structured ions has been reported and compared with calculations of Gillespie for H, He, and Li projectiles. Theory and experiment have been found to agree within the limits of experimental uncertainty so that the extensions of the Bethe theory to a simple target system seem to be on firm foundations.

Equivelocity isoelectronic heavier ions of the present study cannot be incorporated into the above scheme since the interaction is no longer adequately described by the first-order Born approximation. The parameter κ, characterizing the Coulomb interaction and scaling as q/v, requires very large energies to achieve asymptotic conditions for the highly charged species. However, these cases have been described in an approximate fashion; first by the qualitative considerations of Bohr, who associated the decrease in the cross section compared to the Bethe result with the decrease in the importance of resonant collisions, and second by the three-state close-coupling approach of Janev, who introduces an effective continuum oscillator strength.

These theories serve to describe the transition to the cross-section maximum most appropriately for highly charged ions in an approximate but highly descriptive way. Coincidence measurements, which separated the electron loss from helium into pure ionization and capture to bound states, lend considerable support to Janev's absolute universal curve for ionization of this target in the intermediate regime. However, problems associated with the description of ionization of atomic hydrogen are noted, and in particular, the role of charge transfer to the continuum, not explicitly accounted for in Janev's treatment, is pointed out.

Finally, some comments are in order concerning the general scope of the study. The work has focused on the limits of the applicability of the Born approximation for the description of the total-ionization cross section by fast, light ions. A specialist, who deals with differential cross sections for specific excitation and ionization processes, may term the Born approximation as a poor theoretical approach since it inevitably fails to describe certain specific phenomena of a special character. What needs to be emphasized, however, is that the Bethe theory provides an excellent framework for the majority of inelastic phenomena in high-velocity atomic collisions, excused as it were, by the generality of its scope and simplicity of character, which is essentially spectroscopic. Whenever one attempts to account for the phenomena of a special nature, and in particular, those

which form a small contribution to the sum of inelastic phenomena, the inadequacy of the Born approximation may well become apparent. This is precisely the subject of part II of this study, where the charge-state scaling of multiple ionization of noble gases is investigated for a wide range of charge states and velocities of heavy incident projectiles.

ACKNOWLEDGMENTS

We are very grateful to Mitio Inokuti for his communications during the course of this work as well as for his detailed comments on the manuscript. However, this does not imply that he may necessarily approve of all of the points contained in the final form.

---

[1]H. Bethe, Ann. Phys. (Leipzig) 5, 325 (1930).
[2]M. Inokuti, Rev. Mod. Phys. 43, 297 (1971).
[3]M. Inokuti, Argonne National Laboratory Report No. ANL-76-88-I, 177 (unpublished).
[4]V. S. Nikolaev, V. S. Senashenko, V. A. Sidovic, and V. Yu. Shafer, Zh. Tekh. Fiz. 48, 1399 (1978) [Sov. Phys.—Tech. Phys. 23, 789 (1978)].
[5]George H. Gillespie, Phys. Lett. 72A, 329 (1979).
[6]R. K. Janev and L. P. Presnyakov, J. Phys. B 13, 4233 (1980).
[7]J. Lindhard, Nucl. Instrum. Methods 132, 1 (1976).
[8]P. Hvelplund, H. K. Haugen and H. Knudsen, Phys. Rev. A 22, 1930 (1980).
[9]H. S. W. Massey and H. B. Gilbody, in *Electronic and Ionic Impact Phenomena* (Clarendon, Oxford, 1974), Vol. IV, p. 2659.
[10]H. B. Gilbody and J. B. Hasted, Proc. R. Soc. London, Sect. A 240, 382 (1957).
[11]M. Kaminsky, in *Atomic and Ionic Impact Phenomena on Metal Surfaces* (Springer, Berlin, 1965), Sec. 12.2.2.
[12]Reference 9, p. 2549.
[13]H. K. Haugen, L. H. Andersen, P. Hvelplund, and H. Knudsen, Phys. Rev. A 26, 1962 (1982).
[14]M. L. Ter-Mikaelian, *High Energy Electromagnetic Processes in Condensed Media* (Wiley-Interscience, New York, 1972).
[15]N. Bohr, K. Dan. Vidensk. Selsk. Mat.-Fys. Medd. 18, No. 8 (1948).
[16]N. Bohr, Philos. Mag. 25, 10 (1913).
[17]R. K. Janev (unpublished).
[18]P. Hvelplund, J. Phys. B 9, 1555 (1976).
[19]R. E. Olson, Phys. Rev. A 18, 2464 (1978).
[20]M. B. Shah and H. B. Gilbody, J. Phys. B 14, 2831 (1981).
[21]R. E. Olson and A. Salop, Phys. Rev. A 16, 531 (1977).
[22]R. Shakeshaft, Phys. Rev. A 18, 1930 (1978).

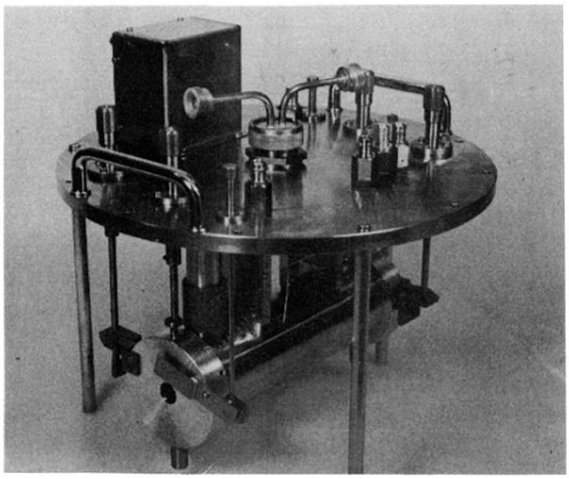

FIG. 2. Photograph of gas cell.